Spatial Organization of Hominin Activities at Gesher Benot Ya'aqov, Israel

Nira Alperson-Afil, *et al.*

Science **326**, 1677 (2009);
DOI: 10.1126/science.1180695

to the midplane (*17*). However, for wet disks, the energetic photons that normally heat the disk via photoelectric heating are now also absorbed by H_2O in the dust-poor atmosphere. This changes the characteristics of the gas and dust heating; the primary heating agents can now be the hot photoproducts of the photodissociated water (OH, O, and H). Laboratory experiments and theoretical modeling of photoexcited water suggest that as much as 50 to 70% of the photon energy will be deposited locally in the disk atmosphere as heat (*18*). The remainder is radiated by highly rotationally excited and superthermal OH in its ground electronic state at wavelengths between 10 and 30 μm (*19*). This line radiation provides a nonlocal source of heating deeper in the disk, perhaps down into the planet-forming zone. Furthermore, in disks for which FUV radiation is the principal gas-heating agent, the buildup of a sufficiently large column density of water will be the main factor limiting the extent of the warm layer. Thus, in disks where the thermodynamics are strongly coupled to the water chemistry, the onset of water self-shielding will truncate the warm layer at a depth corresponding to $\tau_{H_2O} \cong$ few. A limit is therefore imposed on the column density of warm water; in effect, the water becomes a victim of its own success. Despite this effect, the cold water near the midplane will still be shielded and may even initiate its own vigorous self-shielding. The observations are consistent with this possibility (warm $\tau_{H_2O} \leq$ few), although the precise roles played by the main disk-heating agents (for example, FUV and x-rays) are still largely unknown (*20*). Recently, water formation has been independently examined in an x-ray–dominated disk with no FUV (*21*). Those models can produce the observed water column densities, but they are deficient in OH. Our water self-shielding mechanism is able to match both. Even in dust-rich disks, water can provide an additional source of UV opacity and contribute to disk heating.

The persistence of water vapor in our models suggests that it is unlikely to be a transient phenomenon and may be present during the era of planet formation. It also shows that gaseous water vapor originating from evaporating icy planetesimals (*22*, *23*) is not the sole mechanism that can match astronomical observations. Similar to the ozone layer that protects Earth's surface from the destructive effects of solar UV radiation, water created in situ at the disk surface within a few astronomical units of the star will protect any water vapor either created via gas-phase reactions or supplied to the midplane via evaporating icy planetesimals. In addition, the surface water will protect any molecules created by gas-phase chemistry, allowing for a rich organic chemistry to persist in the inner few astronomical units, even as the dust grains evolve toward planets (*3*, *24*). Some of this water and organic material could potentially be incorporated into nascent Earth-like worlds (*25*, *26*).

References and Notes

1. C. P. Dullemond, C. Dominik, *Astrophys. J.* **434**, 971 (2005).
2. J. R. Najita, J. S. Carr, A. Glassgold, J. Valenti, *Protostars and Planets V*, B. Reipurth, D. Jewitt, K. Keil, Eds. (Univ. of Arizona Press, Tucson, AZ, 2007), pp. 507–522.
3. J. S. Carr, J. R. Najita, *Science* **319**, 1504 (2008).
4. C. Salyk *et al.*, *Astrophys. J.* **676**, 49 (2008).
5. E. F. van Dishoeck, A. Dalgarno, *Astrophys. J.* **277**, 576 (1984).
6. K. Yoshino, J. R. Esmond, W. H. Parkinson, K. Ito, T. Matsui, *Chem. Phys.* **211**, 387 (1996).
7. D. L. Baulch, *Evaluated Kinetic Data for High Temperature Reactions* (CRC Press, Cleveland, OH, 1972).
8. T. Joseph, D. G. Truhlar, B. C. Garrett, *J. Chem. Phys.* **88**, 6982 (1988).
9. Materials and methods are available as supporting material on *Science* Online.
10. E. A. Bergin, Y. Aikawa, G. A. Blake, E. F. van Dishoeck, *Protostars and Planets V*, B. Reipurth, D. Jewitt, K. Keil, Eds. (Univ. of Arizona Press, Tucson, AZ, 2007), chap. 8.
11. N. Grevesse, M. Asplund, A. J. Sauval, *Space Sci. Rev.* **130**, 105 (2007).
12. L. Hartmann, *Accretion Processes in Star Formation* (Cambridge Univ. Press, Cambridge, 2001).
13. E. I. Chiang, P. Goldreich, *Astrophys. J.* **490**, 368 (1997).
14. S. J. Weidenschilling, J. N. Cuzzi, *Protostars and Planets III*, E. Levy, J. I. Lunine, Eds. (Univ. of Arizona Press, Tucson, AZ, 1993), pp. 1031–1060.
15. E. Furlan *et al.*, *Astrophys. J. Suppl. Ser.* **165**, 568 (2006).
16. E. F. van Dishoeck, J. H. Black, *Astrophys. J.* **334**, 771 (1988).
17. B. Jonkheid, C. P. Dullemond, M. R. Hogerheijde, *Astron. Astrophys.* **463**, 203 (2007).
18. D. H. Mordaunt, M. N. R. Ashford, R. N. Dixon, *J. Chem. Phys.* **100**, 7360 (1994).
19. A. Tappe, C. J. Lada, J. H. Black, A. A. Muench, *Astrophys. J.* **680**, 117 (2008).
20. A. E. Glassgold, J. Najita, J. Igea, *Astrophys. J.* **615**, 972 (2004).
21. A. E. Glassgold, R. Meijerink, J. R. Najita, *Astrophys. J.* **701**, 142 (2009).
22. F. J. Ciesla, J. N. Cuzzi, *Icarus* **181**, 178 (2006).
23. F. J. Ciesla, *Science* **318**, 613 (2007).
24. M. Agundez, J. Cernicharo, J. R. Goicoechea, *Astron. Astrophys.* **483**, 831 (2008).
25. M. Stimpfl, A. M. Walker, M. J. Drake, N. H. de Leeuw, P. Deymier, *J. Cryst. Growth* **294**, 83 (2006).
26. M. Ikoma, H. Genda, *Astrophys. J.* **648**, 696 (2006).

27. We gratefully acknowledge funding by NASA under grant NN08 AH23G from the Astrophysics Theory and Fundamental Physics and Origins of Solar System programs.

Supporting Online Material

www.sciencemag.org/cgi/content/full/326/5960/1675/DC1
Materials and Methods
Figs. S1 and S2
References

27 May 2009; accepted 22 October 2009
10.1126/science.1176879

Spatial Organization of Hominin Activities at Gesher Benot Ya'aqov, Israel

Nira Alperson-Afil,[1]* Gonen Sharon,[1] Mordechai Kislev,[2] Yoel Melamed,[2] Irit Zohar,[3,4,5] Shosh Ashkenazi,[5] Rivka Rabinovich,[1,5] Rebecca Biton,[5] Ella Werker,[6] Gideon Hartman,[7] Craig Feibel,[8] Naama Goren-Inbar[1]*

The spatial designation of discrete areas for different activities reflects formalized conceptualization of a living space. The results of spatial analyses of a Middle Pleistocene Acheulian archaeological horizon (about 750,000 years ago) at Gesher Benot Ya'aqov, Israel, indicate that hominins differentiated their activities (stone knapping, tool use, floral and faunal processing and consumption) across space. These were organized in two main areas, including multiple activities around a hearth. The diversity of human activities and the distinctive patterning with which they are organized implies advanced organizational skills of the Gesher Benot Ya'aqov hominins.

Ethnographic data of modern hunter-gatherers suggest that their activities are spatially patterned (*1*). Accordingly, the organization of activities across space is often associated with modern humans and is thus considered to reflect modern behavior (*2*, *3*). Attempts to trace the origins of this behavior have concentrated on spatial analyses of Middle Stone Age/Middle Paleolithic sites in Africa (*3*), Europe (*4*), and the Levant (*5*, *6*). Spatial analyses of archaeological sites offer insight into past human activities, behavior, and cognition and provide evidence of how hominins perceived their living space, functionally and/or socially. Here, we present a spatial analysis of an Acheulian occupational level from

[1]Institute of Archaeology, Hebrew University of Jerusalem, Mount Scopus, Jerusalem 91905, Israel. [2]Faculty of Life Sciences, Bar-Ilan University, Ramat-Gan 52900, Israel. [3]Leon Recanati Institute for Maritime Studies, University of Haifa, Mount Carmel, Haifa 31905, Israel. [4]Department of Zoology, George S. Wise Faculty of Life Sciences, Tel Aviv University, Tel Aviv 69978, Israel. [5]National Natural History Collections, Hebrew University of Jerusalem, Givat Ram, Jerusalem 91904, Israel. [6]Department of Botany, Hebrew University of Jerusalem, Givat Ram, Jerusalem 91904, Israel. [7]Department of Human Evolution, Max Planck Institute for Evolutionary Anthropology, Deutscher Platz 6, 04103 Leipzig, Germany. [8]Department of Geological Sciences, Rutgers University, New Brunswick, NJ 08901, USA.

*To whom correspondence should be addressed. E-mail: alperson@mscc.huji.ac.il (N.A.-A.); goren@cc.huji.ac.il (N.G.-I.)

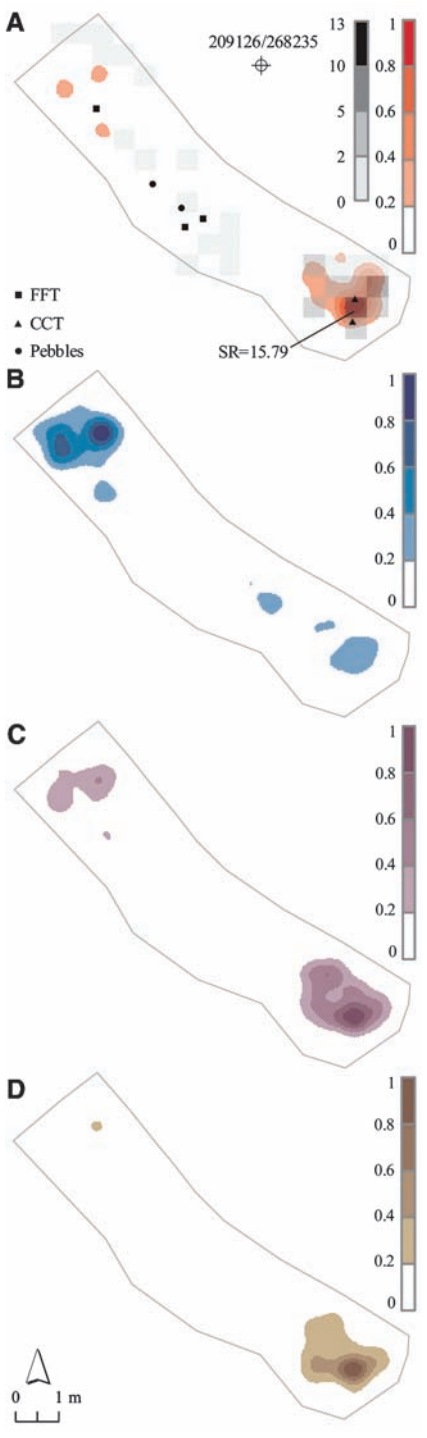

Fig. 1. Kernel density maps of microartifacts in Level 2. (**A**) Burned flint microartifacts (N = 563). Shown are excavated units in which the observed percentage of burned microartifacts exceeds the expected percentage (gray-to-black scale); significant Standardized Residuals (SR) values (*17*); and the distribution of large burned flint items [flakes and flake tools (FFT), N = 3; cores and core tools (CCT), N = 2; pebbles, N = 2]. (**B**) Unburned flint microartifacts (N = 73,064). (**C**) Basalt microartifacts (N = 3889). (**D**) Limestone microartifacts (N = 2154). (A map reference to the Israel Grid, coordinates to the nearest meter, appears at the top of all figures.)

Gesher Benot Ya'aqov, which shows that some early humans were organizing their living spaces by 790,000 years ago.

Gesher Benot Ya'aqov is located on the shores of the paleo–Lake Hula in the northern Jordan Valley in the Dead Sea Rift (*7*). The Early to Middle Pleistocene sediments document an oscillating freshwater lake and represent some 100,000 years of hominin occupation (Oxygen Isotope Stages 18–20) dating to 790,000 years ago (*8*, *9*). Fourteen archaeological horizons indicate that Acheulian hominins repeatedly occupied the lake margins, where they skillfully produced stone tools, systematically butchered and exploited animals, gathered plant food, and controlled fire (*7*, *10*–*15*).

We focus on a hearth area and the lithic, botanical, and paleontological assemblages of Layer II-6 Level 2 (henceforth Level 2), one of eight superimposed occupational levels in Layer II-6. This sedimentary sequence was rapidly sealed, preserving the original location of different artifacts (evidenced by the fresh preservation state of the lithics, the preservation of mollusk embryos, the presence of conjoinable bones, and a lack of winnowing) (*8*, *10*, *15*, *16*). Level 2 is 0.12 m thick, and we excavated across an area of 25.6 m^2 (3 m^3). It yielded numerous stone artifacts made of different raw materials; a large assemblage of wood, bark, fruits, seeds, and nuts; and highly diverse lacustrine and terrestrial animal remains.

Phantom hearths could be identified by the spatial distribution of small burned debris (*15*). The flint items from Level 2 exhibit low frequencies of burning (table S1): only 0.76% of the microartifacts and 1.05% of the macroartifacts (*17*). Although unburned flint microartifacts occur mostly in the northwestern area, most of the burned ones are concentrated in 3.25 m^2 in the southeast (Fig. 1 and fig. S1). Close to 60% of the burned flint microartifacts, but only 22% of the unburned ones, occur within this limited area (*17*).

The concentration of burned flint microartifacts reflects a knapping activity area near a hearth. A variety of parameters (*15*) support the interpretation of an anthropogenic fire rather than a natural one. In addition, wood segments in Level 2 are abundant but rarely burned: Only two (2.63%

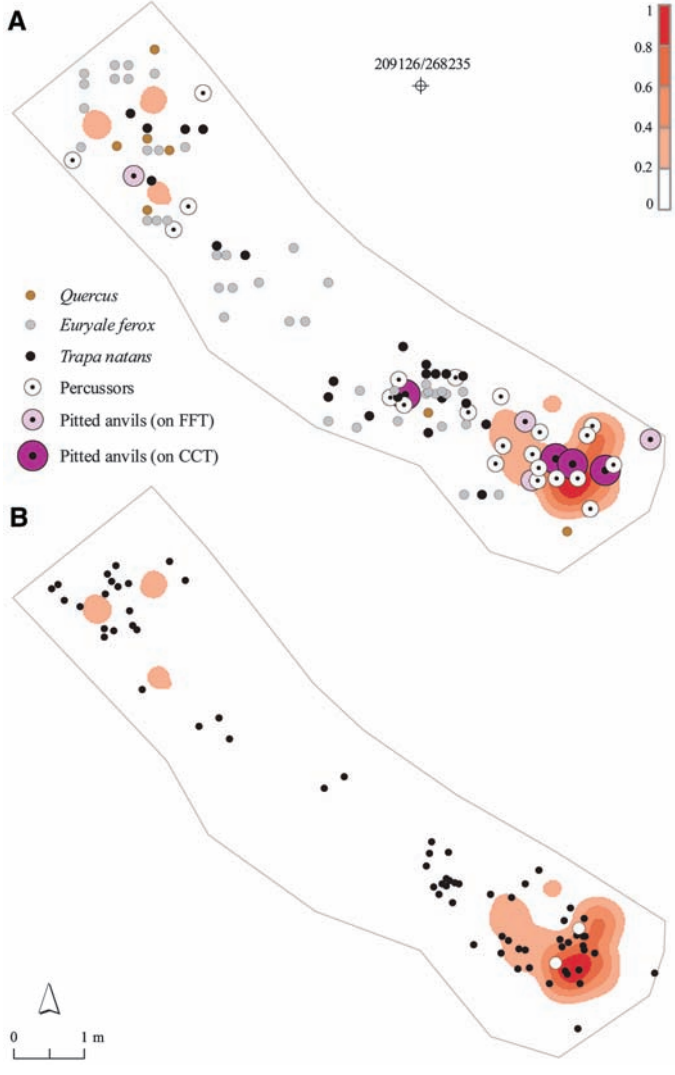

Fig. 2. (**A**) The distribution of pitted stones (N = 8), percussors (N = 22), and *Euryale ferox* (N = 41), *Trapa natans* (N = 22), and *Quercus* (N = 7) nuts in Level 2, superimposed on the kernel density map of burned flint microartifacts (N = 563). (**B**) Distribution of wood pieces (N = 74); the two burned pieces are marked in white.

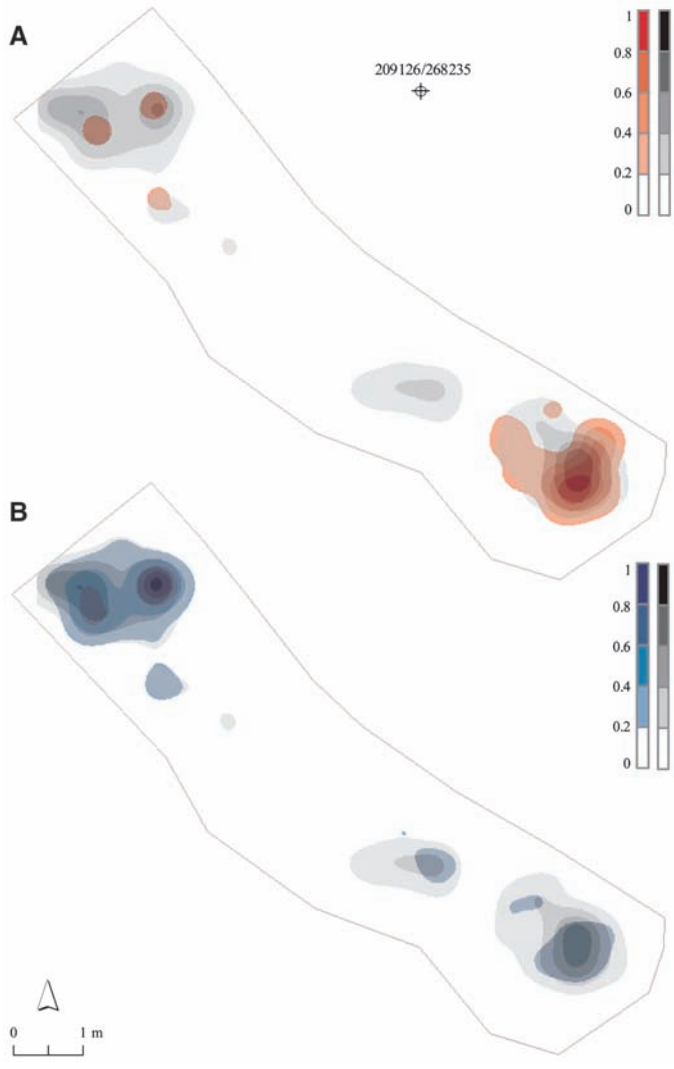

Fig. 3. Kernel density map of the distribution of fish remains (N = 2457) in Level 2, slightly transparent and superimposed on the kernel density map of (**A**) burned flint microartifacts; (**B**) unburned flint microartifacts.

of the wood assemblage), in spatial association with the hearth area, are burned (Fig. 2). Among the smaller botanical remains (grains, fruits, seeds, and wood pieces smaller than 2 cm), burning frequencies are 3.4% (8 of 238). Low frequencies of burning are also recorded for the different flint artifacts (table S1). Burning of flint artifacts at Gesher Benot Ya'aqov required a high temperature (above 350°C) and direct contact with the flints (*18*, *19*).

The lithic assemblage of Level 2 comprises 79,670 microartifacts and 1412 macroartifacts (table S1). Kernel density maps of flint, basalt, and limestone microartifacts reveal that flint knapping was carried out mostly in the northwestern area and, to some extent, near the hearth (Fig. 1 and fig. S1). In contrast, basalt and limestone are concentrated in the southeastern area (Fig. 1 and fig. S1). Several bifaces were recovered close to the hearth and most were some 2 m to the northwest (fig. S2). Soft hammer knapping, often linked with biface production (*20*), also seems to be associated with the hearth area, as evidenced by the typical traits observed on basalt and flint flakes (e.g., lipped striking platforms) (*21*), most of which occur close to the hearth (fig. S2).

Some tool types (e.g., notches and denticulates) were distributed throughout the excavated area, but others were most abundant within 1 m of the hearth (fig. S3 and table S2). Several basalt and limestone artifacts bear pits of various quantities, sizes, and depths, interpreted as resulting from the recurrent cracking of hard nuts (*12*). Seven of the eight pitted stones occur near the hearth (Fig. 2). A similar distribution is observed for percussors (hammerstones): 18 of 22 are located near the hearth (Fig. 2).

The botanical assemblage (table S3) comprises 61 wood fragments (larger than 2 cm) and 13 pieces of bark. Thirteen wood taxa are identified, including Syrian ash (*Fraxinus syriaca*), olive (*Olea europaea*), and Kermes oak (*Quercus calliprinos*). More than 200 seeds and fruits represent 19 different taxa. Although most taxa indicate wet habitats (e.g., lakes, lake margins, swamps, and near streams), the abundant fruit remains of woodland species such as olive, oak, and officinal storax (*Styrax officinalis*) imply human involvement, as their habitat was likely located some distance from the lake shore. Edible plants include oak acorns, prickly water lily (*Euryale ferox*) seeds, and water chestnut (*Trapa natans*) fruits; these were probably staple foods because of the nutritive value of their starchy nuts. Through roasting, the inedible shell of the nuts can easily be peeled and the tannin content of the acorns reduced. The fruits of the wild grapevine (*Vitis sylvestris*) and olive, and the leaves of the white beet (*Beta vulgaris*) and holy thistle (*Silybum marianum*), may also have been consumed. Because of their low specific gravity and the proximity of the occupations to water, plant pieces smaller than 20 mm (i.e., seeds and fruits) cannot serve as a reliable spatial indicator. Most wood pieces were near the hearth, and the two burned specimens were located within it (Fig. 2).

We recovered remains of various aquatic and terrestrial species (tables S4 and S5). The 17 crab specimens [minimum number of individuals (MNI) = 4 (*22*)], identified as the extant *Potamon potamios*, include pieces of the two asymmetric chelipeds, each with a distinctive form of the movable (upper) and fixed (lower) pincer. Pincers, being thicker and denser than other body parts, constitute 76.5% of the assemblage (table S4). Five display features that permit estimation of the carapace height (*22*) as 23.0 to 48.8 mm, characteristic of medium- and large-sized crabs. Of the seven pincers of the large cheliped present in Level 2, six occur around the hearth. These are the only crab remains in this area (fig. S4) (*23*).

The abundant fish remains [number of identified specimens (NISP) > 2500] (table S5) include three of the five freshwater fish families native to Lake Hula (*24*, *25*). Cyprinidae (carps) predominate (99%) with five identified species, including endemic species (e.g., *Mirogrex hulensis*). Most (62.1%; N = 1602) consist of the extinct large (longer than 1 m) *Barbus* sp. nov. The preservation of fish bones is poor, exhibiting a preponderance of molariform and pharyngeal teeth (99%) and a paucity of other skeletal elements (16 identified skeletal elements out of the more than 70 bones of a complete fish) (table S6). Most of the molariform teeth (>80%) and the fin spines (>60%) are highly fragmented, with less than 40% of the original element present. The fish remains are clumped [Morisita Index of Dispersion; I_d = 3.5, M_u = 0.99, M_c = 1.0071, I_p = 0.5292; see (*17*)] in two concentrations: one in the northwest and one in the southeast, where the hearth is located (Fig. 3). Considering the significant difference between the Level 2 fish assemblage and that of a natural-death assemblage (*26*, *27*) (table S7; χ^2 by randomization: df = 20, χ^2 = 1878.797, $P < 0.0001$), we conclude that the fish assemblage of Level 2 is of anthropogenic origin, demonstrating that this resource was another component of the hominin dietary spectrum. These conclusions are strengthened by the spatial distribution of fish remains, which overlap the activity areas illustrated by the lithics (Fig. 3).

Other faunal remains include freshwater turtles (*28*) and medium- and large-sized mammals (fig.

S4). The latter (N = 27) comprise fallow deer, elephant, and bone fragments assigned to general categories (e.g., artiodactyls, canids, and unidentified mammals). Rodent teeth (N = 22) were also recovered, mainly of *Microtus* (table S4). The mammals' spatial distribution reveals no distinct patterns (fig. S4).

Analyses of Level 2 indicate that hominins carried out different activities in two distinct locations. Abundant flint knapping took place in the northwestern area, resulting in a dense concentration of microartifacts (Fig. 1 and fig. S1). Other noteworthy aspects of this activity area include fish exploitation (Fig. 3) and the use of chopping tools (fig. S3).

Greater variation was seen in the activities carried out near the hearth. Although flint knapping around the hearth was less intensive, basalt and limestone knapping was spatially restricted to the hearth (Fig. 1 and fig. S1). The hearth area also served as a focal point for biface modification and for activities involving the use of chopping tools, side scrapers, end scrapers, and awls (fig. S3). The percussors and the pitted stones suggest that nut processing may have involved the use of fire, as recorded for modern hunter-gatherer societies (*1*, *29*). In addition, the differential preservation of fish and crabs, along with their spatial distribution, suggests that they were consumed near the hearth.

The spatial organization of hominin activities in Level 2 thus resulted in discrete patterning of various categories of finds. The evidence from Gesher Benot Ya'aqov suggests that early Middle Pleistocene hominins carried out different activities at discrete locations. The designation of different areas for different activities indicates a formalized conceptualization of living space, often considered to reflect sophisticated cognition and thought to be unique to *Homo sapiens* (*3*). Modern use of space requires social organization and communication between group members, and is thought to involve kinship, gender, age, status, and skill (*2*).

References and Notes

1. L. R. Binford, *In Pursuit of the Past: Decoding the Archaeological Record* (Thames and Hudson, London, 1983).
2. L. Wadley, *Camb. Archaeol. J.* **11**, 201 (2001).
3. S. McBrearty, A. S. Brooks, *J. Hum. Evol.* **39**, 453 (2000).
4. M. Vaquero, I. Pasto, *J. Archaeol. Sci.* **28**, 1209 (2001).
5. N. Alperson-Afil, E. Hovers, *Euras. Prehist.* **3**, 3 (2005).
6. J. D. Speth, E. Tchernov, in *The Middle Paleolithic Archaeology of Kebara Cave*, O. Bar-Yosef, L. Meignen, Eds. (Peabody Museum of Archaeology and Ethnology, Harvard University, Cambridge, MA, 2007), pp. 165–260.
7. N. Goren-Inbar *et al.*, *Science* **289**, 944 (2000).
8. C. S. Feibel, in *Sediments in Archaeological Contexts*, J. K. Stein, W. R. Farrand, Eds. (Univ. of Utah Press, Salt Lake City, 2001), pp. 127–148.
9. C. S. Feibel, in *Human Paleoecology in the Levantine Corridor*, N. Goren-Inbar, J. D. Speth, Eds. (Oxbow, Oxford, 2004), pp. 21–36.
10. N. Goren-Inbar, A. Lister, E. Werker, M. Chech, *Paléorient* **20**, 99 (1994).
11. N. Goren-Inbar, E. Werker, C. S. Feibel, *The Acheulian Site of Gesher Benot Ya'aqov. The Wood Assemblage* (Oxbow, Oxford, 2002), vol. I.
12. N. Goren-Inbar, G. Sharon, Y. Melamed, M. Kislev, *Proc. Natl. Acad. Sci. U.S.A.* **99**, 2455 (2002).
13. R. Rabinovich, S. Gaudzinski-Windheuser, N. Goren-Inbar, *J. Hum. Evol.* **54**, 134 (2008).
14. N. Goren-Inbar *et al.*, *Science* **304**, 725 (2004).
15. N. Alperson-Afil, *Quat. Sci. Rev.* **27**, 1733 (2008).
16. S. Ashkenazi, K. Klass, H. K. Mienis, B. Spiro, R. Abel, *Lethaia* 10.1111/j.1502-3931.2009.00178.x (2009).
17. See supporting material on *Science* Online.
18. B. A. Purdy, in *Lithic Technology: Making and Using Stone Tools*, E. Swanson, Ed. (Mouton, Paris, 1975), pp. 133–141.
19. J. Sergant, P. Crombe, Y. Perdaen, *J. Archaeol. Sci.* **33**, 999 (2006).
20. B. Madsen, N. Goren-Inbar, *Euras. Prehist.* **2**, 3 (2004).
21. G. Sharon, N. Goren-Inbar, *J. Isr. Prehist. Soc.* **28**, 55 (1999).
22. S. Ashkenazi, U. Motro, N. Goren-Inbar, R. Biton, R. Rabinovich, *J. Archaeol. Sci.* **32**, 675 (2005).
23. Medium- and large-sized crabs often indicate selection for consumption; see (*30*).
24. M. Goren, R. Ortal, *Biol. Conserv.* **89**, 1 (1999).
25. C. Dimentman, H. J. Bromley, D. F. Por, *Lake Hula: Reconstruction of the Fauna and Hydrobiology of a Lost Lake* (Israel Academy of Sciences and Humanities, Jerusalem, 1992).
26. I. Zohar *et al.*, *Palaeogeogr. Palaeoclimatol. Palaeoecol.* **258**, 292 (2008).
27. R. L. Elder, G. R. Smith, *Palaeogeogr. Palaeoclimatol. Palaeoecol.* **62**, 577 (1988).
28. The remains of freshwater turtles (*Mauremys caspica*) (NISP = 3, MNI = 2) (table S4) consist of costals (carapace bony plates). Two fragments belong to adult turtles, whereas the third belongs to a juvenile. The small size of the sample precludes further conclusions and its distribution reveals no distinct patterns (fig. S4).
29. J. E. Yellen, *Archaeological Approaches to the Present: Models for Reconstructing the Past* (Academic Press, New York, 1977).
30. S. Ashkenazi, A. D. Huertas, B. Spiro, *J. Isr. Prehist. Soc.* **37**, 135 (2007).

31. Supported by Israel Science Foundation grant 300/06 to the Center of Excellence Project "The Effect of Climate Change on the Environment and Hominins of the Upper Jordan Valley between ca. 800 ka and 700 ka as a Basis for Prediction of Future Scenarios." The study of burned flint microartifacts was supported by grants from the German-Israeli Foundation (GIF I-896-208.4/2005) and the Israel Science Foundation (886/02). The study of fish remains was supported by the Irene Levi Sala CARE Archaeological Foundation and carried out at the Department of Zoology and the I. Meier Segals Garden for Zoological Research at Tel Aviv University and at the Natural History Museum (NHM) in London and Brussels. We thank M. Goren for his help and support in the study and collection of freshwater fish; W. Van Neer (NHM Brussels), M. Richter, P. Campbell, and O. Crimmen (NHM UK) for providing access to labs and collections as well as helpful comments; A. Ben-Nun, head of the GIS center at the Hebrew University of Jerusalem, and I. Sharon and I. Gilead for greatly assisting in establishing the methodology for this study; M. Haber and S. Gorodetsky, who edited the manuscript with their usual professionalism; and two anonymous reviewers for their constructive and helpful comments.

Supporting Online Material

www.sciencemag.org/cgi/content/full/326/5960/1677/DC1
Materials and Methods
Figs. S1 to S4
Tables S1 to S7
References

17 August 2009; accepted 13 October 2009
10.1126/science.1180695

Mozambican Grass Seed Consumption During the Middle Stone Age

Julio Mercader

The role of starchy plants in early hominin diets and when the culinary processing of starches began have been difficult to track archaeologically. Seed collecting is conventionally perceived to have been an irrelevant activity among the Pleistocene foragers of southern Africa, on the grounds of both technological difficulty in the processing of grains and the belief that roots, fruits, and nuts, not cereals, were the basis for subsistence for the past 100,000 years and further back in time. A large assemblage of starch granules has been retrieved from the surfaces of Middle Stone Age stone tools from Mozambique, showing that early *Homo sapiens* relied on grass seeds starting at least 105,000 years ago, including those of sorghum grasses.

The Mozambican cave site of Ngalue (12°51.517′S, 35°11.902′E) is part of the Niassa Rift (Fig. 1). The cave formed in Proterozoic carbonate rocks (*1*) located at 1300 m above sea level. There is a 20-m-long corridor leading into dark chambers, which have the most habitable space, with a useable floor area covering >50 m^2 and a ceiling height of ~8 m. The portion of the sequence and the artifacts studied here were deposited throughout the so-called "Middle Beds" (*2*), a Middle Stone Age clast-supported and time-averaged unit with light yellowish brown sediments that are rich in angular cave spall, lithics, animal bones, and teeth. The deposits span a time range from 105,000 to 42,000 years ago (*2*). Excavation in 2007 retrieved 555 quartz artifacts.

For this study, I chose 70 stone tools (~12% of the Middle Stone Age assemblage) from all main technotypological types to take into account the broadest range of potential plant uses: scrapers (35%), core tools/grinders (25%), points (15%), flakes (7%), and miscellaneous tools (18%) (Table 1). I selected tools from across the entire industrial scatter across a 13-m transect running along the largest cave chamber. These include

Department of Archaeology, University of Calgary, Alberta, T2N 1N4, Canada.

Supporting Online Material for

Spatial Organization of Hominin Activities at Gesher Benot Ya'aqov, Israel

Nira Alperson-Afil,* Gonen Sharon, Mordechai Kislev, Yoel Melamed, Irit Zohar, Shosh Ashkenazi, Rivka Rabinovich, Rebecca Biton, Ella Werker, Gideon Hartman, Craig Feibel, Naama Goren-Inbar*

*To whom correspondence should be addressed. E-mail: alperson@mscc.huji.ac.il (N.A.-A.); goren@cc.huji.ac.il (N.G.-I.)

Published 18 December 2009, *Science* **326**, 1677 (2009)
DOI: 10.1126/science.1180695

This PDF file includes:

Supporting Online Material

Materials and Methods

Excavation methods and provenance recording

Excavations at the site of GBY were carried out using a horizontal 1 m^2 grid constructed above the excavated surfaces, and corresponding with the coordinates of the Israel grid. Excavations were conducted along the strike and dip of the layers with the aim of laterally exposing the tilted archaeological horizons (Goren-Inbar et al., 2002: Figures. 4–5); this procedure enabled the detailed representation of the spatial organization of each occupation surface. The standard unit of excavation was thus the tilted projection of a horizontal 1 m^2 grid square. Each horizontal grid square was subdivided into four 0.5 × 0.5 m squares and excavated in spits that covered the area of one sub-square to an average depth of 5 cm. Once exposed, the surface (i.e., the living floor) was drawn and items were retrieved with a full spatial reference (X, Y, and Z); these "coordinated pieces" consist mostly of items larger than 20 mm (i.e., macroartifacts). Other items retrieved during excavation—the "uncoordinated pieces"—were labeled according to the spit's spatial reference (i.e., the excavated unit/sub-square and an elevation range). Such items can thus be located with an exactitude of 0.5 × 0.5 × 0.05 m.

In addition to material retrieved during excavation, the excavated sediments embodying the archaeological horizons were wet-sieved at the site by a 2-mm sieve. The sediments were then bagged with their recorded spit location and transported to the Institute of Archaeology of the Hebrew University for further analysis. Sorting of the sieved sediments yielded rich and varied assemblages, such as fruits, seeds, grains, bones

and teeth of micromammals, fish, and crabs, and specks of charcoal. Most of the small lithic items (basalt, flint, limestone) were retrieved through this procedure, including all items ranging in size from 2 to 20 mm (microartifacts). As the wet-sieved sediments were retrieved from the field with their recorded spit location, these microartifacts can be located with an exactitude of 0.5 × 0.5 × 0.05 m.

Spatial Plotting

A large amount of archaeological material was retrieved with a general spatial reference, either during excavations or through the sorting of the wet-sieved sediments. The sediments' spatial reference includes the X and Y quadrant (0.5 × 0.5 m) and the spit depth (Z is a range of depths). Such spatial recording allows only the representation of relative frequencies per excavated unit. Other spatial analyses, such as creating a density map, would necessitate measuring the distances between different features and thus require that the data be depicted as distinct points.

It has been suggested that assigning a random spatial reference within the excavated area provides a reliable, and almost identical, spatial representation (Gilead, 2002). Taking this into consideration and using the *Visual Basic* language within the *Access* program (Microsoft® Access 2002), items with a general spatial reference were given a new reference point within their recorded sub-square. This procedure enabled the plotting of each excavated find and included several stages.

First, each database (of the different finds categories) was treated separately and sorted according to the recorded excavated units. Each of these excavated units featured a defined excavated area (0.5 × 0.5-m sub-squares or 1 × 1-m squares), from which a

certain amount of items was retrieved. This area (a) was then divided by the maximum value of items retrieved from that area (n) so that each item could be plotted separately within an a/n area (δ). Let us hypothesize a case in which a given 1 m^2 excavated area (a=1) contains 100 flint items (n=100). If these 100 items were distributed *evenly* within the 1 m^2 area, each item would then occupy an area of 1/100 m^2 (δ =0.01). The new reference point for each item is defined as the southwestern corner of each δ cell, so that:

$$a = \sum \delta_{1\text{-}n} \, (\delta_1 + \delta_2 + \delta_3 + \delta_4 \ldots . \delta_n)$$

This procedure enables the items to be plotted *uniformly* within their recorded spit, ensuring that the new plotted data are as consistent as possible with the recorded data of sub-square precision. Other plotting methods (e.g., random plotting) could result in the formation of artificial clusters within the sub-square area.

The assignment of artificial coordinates to the archaeological material enables the various databases to be used as geographical information that can be integrated into GIS software. This package is a collection of software and geographic data for capturing, managing, analyzing, and displaying all forms of geographically referenced information (see: http://www.esri.com/software/arcgis/about/desktop_gis.html). For this study, *ArcMap* software (ESRI®ArcMap™9.3) was used for the spatial display and analyses of the archaeological data. In order to graphically illustrate areas of high density, the point-plotted data of microartifact distribution were converted into kernel density maps.

Kernel density calculates the density of point features around each output cell (determined here as 0.01 m). Conceptually, a smoothly curved surface is fitted over each point. The surface value is highest at the location of the point, and diminishes with

increased distance, reaching 0 at the search radius distance from the point (determined here as 0.5 m). For this reason, only a circular neighborhood is possible. The density value at each output cell is calculated by adding the values of all the kernel surfaces where they overlie the cell center (Silverman, 1986: 76, equation 4.5). Determination of different search radii thus changes the scale of the analysis results. With a smaller radius, fewer points will fall within the search radius, resulting in numerous small, "dense" features. Increasing the radius will result in more points falling within the search radius; when calculating density, the number of points will be divided by a larger area, leading to larger, generalized concentrations. The cell size (0.01 m) and search radius (0.5 m) values were chosen for this study since they closely represent the genuine patterns observed within the schematic illustrations of the data (i.e., frequencies per excavated unit/sub-square). Finally, in order to create a uniform scale (from 0 to 1) that enables comparison between kernel density maps of different data sets (e.g., burned vs. unburned flint), the densities have been standardized by the maximum values of each data set.

Homogeneity Analysis (observed and expected burning) was used in order to examine the distribution of burned microartifacts. This method examines the distribution of the burned flint microartifacts in comparison with that of the unburned ones. In cases of absolute overlap between the distribution of the burned and unburned flint microartifacts, we expect the relative percentage of burned items to be homogeneous across the exposed surface, displaying similar values in each excavated grid unit. Thus, if the general percentage of burned flint microartifacts in a particular layer is 2.00%, we would then expect that within each excavated unit (i.e., 0.5 × 0.5-m sub-squares) the

percentage of burned items within the total flint microartifacts of the sub-square will similarly be 2.00%.

In order to compare the observed and expected percentages of burned items in each excavated unit, the expected percentage of burned flint microartifacts was subtracted from the observed percentage. The value obtained through this calculation is the deviation between the observed and expected percentage of burning in each excavated unit; units of positive values are excavated sub-squares in which the observed percentage of burning exceeds that expected in the case of uniform distribution of the burned flint microartifacts.

Statistical Tests

The GIS package supports various types of spatial statistic tools (e.g., cluster analyses, nearest-neighbor analysis, etc.); however, differentiating between burned and unburned flint patterning is not a straightforward issue. The burned flint microartifacts spatially originate from the larger flint component, which may *a priori* be spatially clustered; we therefore cannot consider the burned flint microartifacts a spatially distinct sample on which spatial statistic analyses can be performed. But had we done so, we would have failed to notice the possible overlap of the burned and unburned flints, which is a fundamental factor in reliable identification of anthropogenic fire. A chi-square test, however, can examine the spatial differences between the burned and unburned flint microartifacts, providing a statistical parameter of probability for that differentiation. The chi-square (χ^2) value was thus calculated for the burned flint microartifacts in all the excavated units (i) by the following equation:

$$\chi^2 = \sum_i \frac{(OBS_i - EXP_i)^2}{EXP_i}$$

so that the absolute chi-square test value of a particular archaeological layer is the summary of χ^2 values of all excavated units (i=number of excavated units).
The probability level (p) of the chi-square test is then extracted by comparing the calculated chi-square value to a critical value from a chi-square table, with degrees of freedom corresponding to that of the data ($df=i-1$).

The chi-square goodness of fit supplies a parameter of differentiation between the observed distribution and an expected, uniform distribution. It does not, however, indicate what is specifically significant. This can be portrayed in the standardized residuals (SR), which are the signed square root of each category's contribution to the χ^2:

$$SR = \frac{OBS_i - EXP_i}{\sqrt{EXP_i}} \sim N(0,1)$$

What the above formula essentially states is that the standardized deviations are approximately (asymptotically) normally distributed; i.e., given a large enough sample and a sufficient number of units, we would expect (under the assumptions of the null hypothesis) that about two-thirds of the units will have SR values in the -1 to +1 range, and about 95% will be between -2 and +2, etc. Thus, any unit for which the SR value is greater than 2 (and the expected value is larger than 5) is considered a substantial contributor to the significance observed in the chi-square test (e.g., Haberman, 1973). Standardized residuals were thus calculated for the burned flint microartifacts. In those cases where the distribution of burned flint microartifacts is significantly different than

that of the unburned ones, we can evaluate the contribution of different excavated areas to the observed difference.

Results of statistical tests

1) The distribution of burned and unburned flint microartifacts

A chi-square test of the distribution of burned flint microartifacts in each excavated unit (0.5 × 0.5-m sub-squares) of Level 2 substantiates the significance of the apparent clustering of burned microartifacts ($\Sigma\chi^2$=913.27; *df*=68; p<0.001). In addition, homogeneity analysis indicates that the percentage of burned flint microartifacts in the sub-square encircling the highest-density kernel is 12.63% higher than what we would expect had the burning distribution been uniform. Similarly, the high significance of the standardized residual test of this sub-square (SR=15.79; N [expected]=20.5) points to this concentration as the major contributor to the observed clustering.

2) The distribution of fish remains

In order to test the bone spatial distribution pattern, we used the standardized Morisita index of dispersion. This is one of the best measures for distribution because it is independent of population density and sample size (Heck et al., 1975; Hurlbert, 1971; Krebs, 1999).

Figures

Fig. S1. The distribution of microartifacts per excavated unit in Level 2. (**A**) Percentage of burned flint microartifacts per excavated unit (N=563). (**B**) Percentage of unburned flint microartifacts per excavated unit (N=73,064). (**C**) Percentage of basalt microartifacts per excavated unit (N=3,889). (**D**) Percentages of limestone microartifacts per excavated unit (N=2,154).

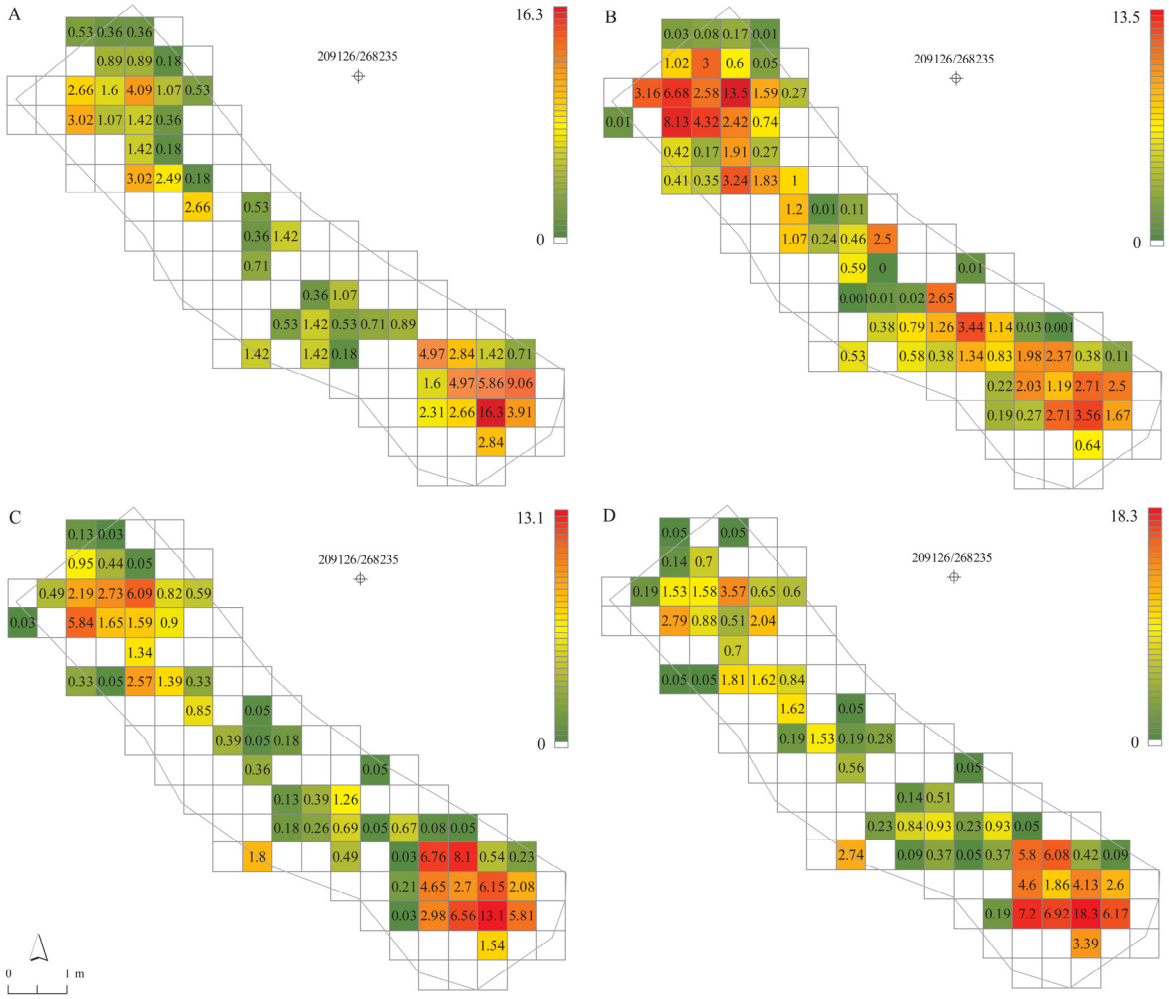

Fig. S2. The distribution of bifacial tools (Handaxes [N=22] and Cleavers [N=10]) and lipped artifacts (N=24) in Level 2, superimposed on the kernel density map of the burned flint microartifacts (N=563).

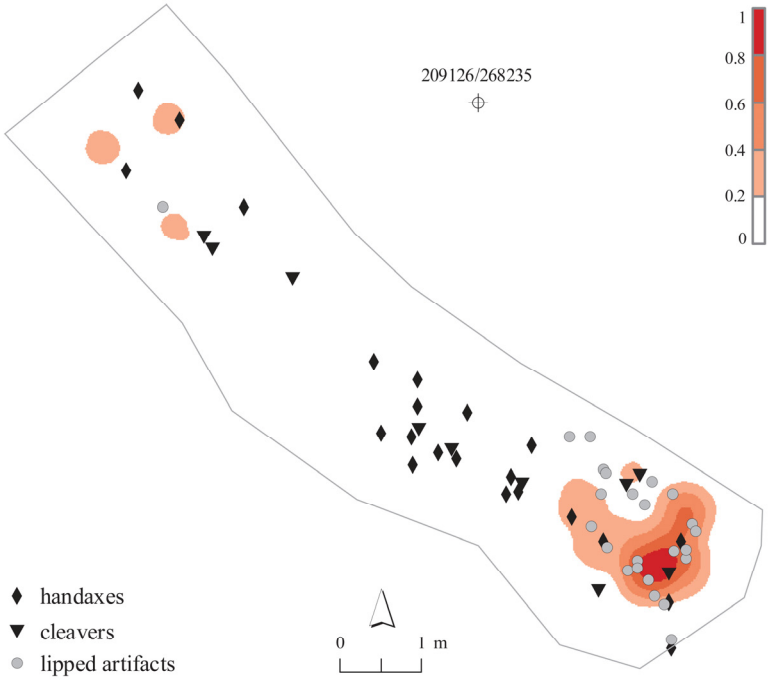

Fig. S3. The distribution of different tool types in Level 2 superimposed on the kernel density map of burned flint microartifacts (N=563). (**A**) Chopping tools (N=20), notches and denticulates (N=46). (**B**) End scrapers (N=13), awls (N=12), burins (N=3), unretouched blades (N=3), and a backed knive (N=1). (**C**) Side scrapers (N=12) and massive scrapers (N=4).

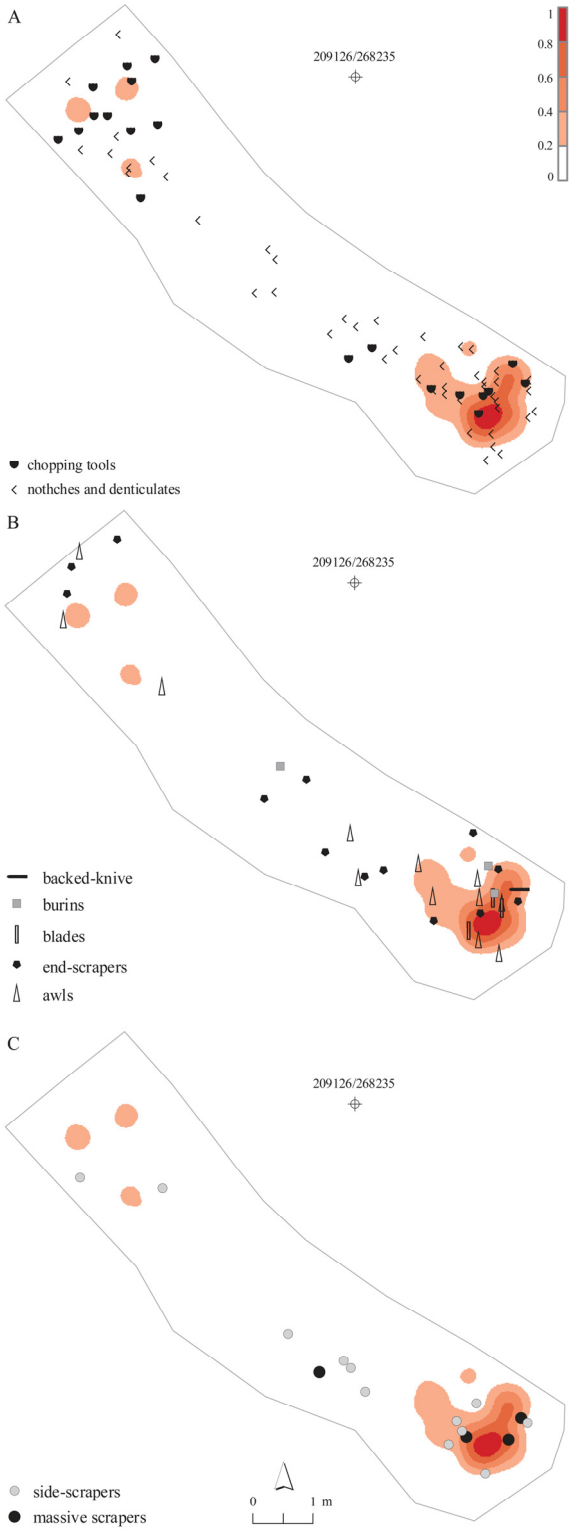

Fig. S4. The distribution of faunal remains in Level 2 superimposed on the kernel density map of the burned flint microartifacts (N=563): medium- and large-sized mammals (N=21), crabs (N=17) (black triangles represent large cheliped pincers), and turtles (N=3).

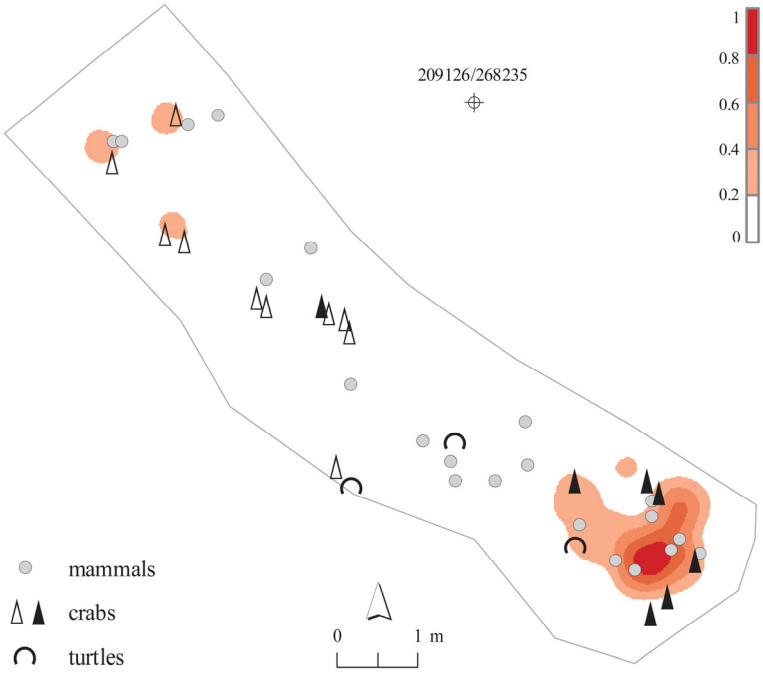

Tables

Table S1. The lithic assemblage of Level 2.

Category	Flint				Basalt	Limestone	Total
	Unburned		Burned				
	(N)	(%)	(N)	(%)	(N)	(N)	(N)
Microartifacts*	73,064	99.23	563	0.76	3,889	2,154	79,670
FFT artifacts*	300	99.00	3	0.99	771	15	1,089
CCT artifacts*	165	98.80	2	1.19	116	8	291
Handaxes	4	-	-	-	18	-	22
Cleavers	-	-	-	-	10	-	10
Pebbles*	792	99.74	2	0.25	875	107	1,776
Total	74,325	99.23	570	0.76	5,679	2,284	82,858

*The percentage of burned and unburned flint items is calculated within each lithic category; FFT=flake and flake tools, CCT=cores and core tools.

Table S2. Frequencies of different tool types in Level 2 including the vicinity of the hearth (1-m radius which covers 3.2 m^2 out of the total 25.6 m^2 of excavated surface).

	Entire level		1-m radius		
	(N)	(%)	(N)	(%)	
				Out of lithic category*	Out of typological group#
Flakes and flake tools (FFT)	1,089	100.00	451	41.41	
Notches and denticulates	46	4.22	22	4.87	47.82
End-notches	10	0.91	3	0.66	30.00
End scrapers	13	1.19	4	0.88	30.76
Burins	3	0.27	2	0.44	66.66
Awls	15	1.37	7	1.55	46.66
Side scrapers	12	1.10	6	1.33	50.00
Massive scrapers	4	0.36	3	0.66	75.00
^Biface-modification flakes	8	0.73	5	1.10	62.50
Backed knife	1	0.09	1	0.22	100.00
Unretouched blades	3	0.27	3	0.66	100.00
Pitted anvils	4	0.36	1	0.22	25.00
Retouched flakes	37	3.39	14	3.10	37.83
Cores and core tools (CCT)	284	100.00	69	24.29	
Pitted anvils	4	1.40	3	4.34	75.00
Chopping tools	20	7.04	9	13.04	45.00
Cores	42	14.78	8	11.59	19.04
Percussors	22	7.74	10	14.49	45.45
Bifacial tools (BF)	32	100.00	8	25.00	
Handaxes	22	68.75	4	50.00	18.18
Cleavers	10	31.25	4	50.00	40.00

*Lithic category: FFT/CCT/BF; #typological group: side scrapers, awls, etc.
^ Including *éclat de taille de biface*.

Table S3. Plant remains from Level 2.

Plant taxon	Common name	Identified part/organ	Range of maximum length (cm)	No. of specimens
Fraxinus syriaca; *Fraxinus*?	Ash	Wood	3.0–20.0	22
Olea europea; *Olea*?	Olive	Wood	4.4–13.8	7
Quercus calliprinos	Kermes oak	Wood	5.0–20.0	5
Lycium	Box-thorn	Wood	1.6–3.2	3
Retama type	White broom	Wood	7.6–11.8	3
Salix sp.; *Salix*?	Willow	Wood	3.2–6.5	3
Populus; *Populus*?	Poplar	Wood	6.2–10.0	2
Pistacia atlantica	Atlantic terebinth	Wood	6.5–8.4	2
Pistacia vera	Pistachio	Wood	4.7	1
Lonicera sp.	Honeysuckle	Wood	3.6	1
Rhus pentaphylla/tripartite	Sumac	Wood	13.0	1
Ulmus sp.	Elm	Wood	4.3	1
Ziziphus/*Paliurus*	Jujube/Christ's thorn	Wood	12.0	1
Bark and bark?	Bark	Bark	2.8–7.0	13
Unidentified		Wood	5.0–21.5	9
Total wood and bark segments				**74**
Adonis sp.	Pheasant's-eye	Fruit		5
Beta vulgaris	White beet	Fruit		3
cf. *Carthamus*	Safflower?	Fruit		1
Euphorbia cf. *valerianifolia*	Spiny fruited sprunge?	Seed		1
Euryale ferox	Prickly water lily	Seed		44
Galium sp.	Bedstraw	Fruit		1
Heliotropium supinum	Trailing heliotrope	Fruit		13
Hymenocarpos circinnatus	Disk trefoil	Pod		1
Lomelosia sp.	Scabious	Calyx		2
Olea europaea	Olive	Stone		35
Potamogeton sp.	Pondweed	Fruit		1
Quercus sp.	Oak	Acorn		6
Quercus sp.	Oak	Cupule		1
Ranunculus cf. *marginatus*	Buttercup	Fruit		10
Ricinus communis	Castor oil plant	Seed		1
Silybum marianum	Holy thistle	Fruit		13
Styrax officinalis	Officinal storax	Stone		28
Trapa natans	Water chestnut	Calyx		22
Vitex sp.	Chaste tree	Drupe		1
Vitis sylvestris	Wild grapevine	Pip		11
Unidentified		Fruit/seed		24
Total fruits and seeds				**224**

Table S4. Faunal remains from Level 2.

Species	Common name	Body element	Maximum length (mm)*	No. of specimens
Freshwater Crabs				
Potamon potamios	Freshwater crab	Large cheliped movable pincer (upper pincer)	5.0–8.5	3
Potamon potamios	Freshwater crab	Large cheliped fixed pincer (lower pincer)	7–17	4
Potamon potamios	Freshwater crab	Unidentified pincer	3–12	6
Potamon potamios	Freshwater crab	Propodus	7	1
Potamon potamios	Freshwater crab	Carapace	6	1
Potamon potamios	Freshwater crab	Maxillary	4–5	2
Reptiles				
Mauremys caspica.	Freshwater turtle	Costal bones, carapace	17.2–23.9	3
Microvertebrates und.	Reptile, microvertebrates	Shaft fragments		6
Mammals				
Canid sp.	-	Tooth fragment	13.65	1
Sus scrofa	Boar	Ulna fragment	85.06	1
Dama sp.	Fallow deer	Antler base, lower Incisor, tooth fragment, second phalanx	14.23–90.07	4
Palaeoloxodon antiquus	Elephant	Skull fragments	14.09–65.57	3
#Body size A	Elephant (?) size	Long bone shaft fragment	145.98	1
#Body size C	Giant deer/Red deer/Boar size	Femur shaft, long bone shaft fragment	66.35	2
#Body size D	Fallow deer size	Teeth fragments	14.54–14.56	2
Unidentified mammal		Splinters	23.56–56.35	12
Micromammals	Rodents	Teeth fragments and postcranials		22
Insectivora und.		Tooth fragment		1

* In cases of more than one specimen the values given are of the range.

Body size A: weight range >1,000 kg; body size C: weight range 80–250 kg; body size D: weight range 40–80 kg (Rabinovich et al., in press).

Table S5. Fish remains from Level 2.

Family	Taxon	Common name	(NISP)	(%)
Cyprinidae	*Carasobarbus canis*	Carp, Binit gdolat kaskas*	88	3.4
	Barbus longiceps	Carp, Binit arukat rosh*	74	2.9
	Large Barbus sp. nov	Large extinct carp	1,602	62.1
	Barbus/Capoeta	Carp	3	0.12
	Capoeta damascina	Carp, Hafaf*	35	1.35
	Mirogrex hulensis	Sardine, Lavnun HaHula*	10	0.4
	Unident. Carp	Carp	742	28.8
Clariidae	*Clarias* sp.	Catfish	1	0.04
Cichlidae	*Tilapia* sp.	St. Peter's fish	23	0.9
Total			2,578	100.00

* In Hebrew

Table S6. Skeletal elements of fish from Level 2 (all taxonomic groups).

Anatomic region	Skeletal element	(NISP)	(%)
Appendicular skeleton	Cleithrum	1	0.04
	Dorsal post-cleithrum	1	0.04
	Supracleithrum	2	0.08
	Pelvic fin	1	0.04
Branchial region	Pharyngeal bone	1	0.04
	Pharyngeal teeth	1,014	39.80
	Molariform teeth	1,509	59.20
Hyoid region	Epihyal	1	0.04
Median fin	Fin ray	1	0.04
	Fin spine	7	0.30
	1st dorsal pterygiophore	2	0.08
	Branchiostegal ray	1	0.04
Opercular series	Opercle	4	0.16
Oromandibular region	Angular/Articular	1	0.04
	Quadrate	1	0.04
Vertebral column	Thoracic vert.	2	0.08
	Precaudal/caudal vert.	1	0.04
Skeleton richness=16/70	Total	2,550	100%

Table S7. Number of Identified Specimens (NISP), taxonomic richness, diversity, number of skeletal elements, and relative abundance of pharyngeal bones and molariform teeth from Level 2 and Area A (natural death assemblage).

Area and Layer	NISP	Taxonomic richness (S)*	Brillouin Index (BH)**	Skeletal elements (N)	Molariform teeth and pharyngeal bones (%)
Area B (II-6 L2)#	2,578	8	1.101	18	90.0
Area A (I-4; I-5)#	1,032	21	3.412	52	20.0

* Taxonomic richness (S)=number of identified species.

** Brillouin index of diversity calculated following Krebs, 1999; Zohar and Belmaker, 2005.

Excavated volume: II-6 Level 2: 3 m^3; Layers I-4 and I-5: 2 m^3.

References

1. I. Gilead, in *Virtual Archaeology*, F. Niccolucci, Ed. (BAR International Series 1075, Arezzo, 2002), pp. 41–43.
2. N. Goren-Inbar, E. Werker, C. S. Feibel, *The Acheulian Site of Gesher Benot Ya'aqov: The Wood Assemblage* (Oxbow Books, Oxford, 2002).
3. S. J. Haberman, *Biometrics* **29**, 205 (1973).
4. K. L. Heck, G. Van Belle, D. Simberloff, *Ecology* **56**, 1459 (1975).
5. S. H. Hurlbert, *Ecology* **52**, 577 (1971).
6. C. J. Krebs, *Ecological Methodology* (Harper Collins Publishers, British Columbia, ed. 2, 1999).
7. R. Rabinovich, S. Gaudzinski-Windheuser, L. Kindler, N. Goren-Inbar, *The Acheulian Site of Gesher Benot Ya'aqov. Mammal Taphonomy – The Assemblages of Layers V-5 and V-6* (Springer, Dordrecht, in press), Vol. III.
8. B. W. Silverman, *Density Estimation for Statistics and Data Analysis* (Chapman and Hall, New York, 1986).
9. I. Zohar, M. Belmaker, *Journal of Archaeological Science* **32**, 635 (2005).